S. Franchini · A. Sanz-Andrés · A. Cuerva

Measurement of velocity in rotational flows using ultrasonic anemometry: the flowmeter

Abstract In this paper a previously developed theoretical model of the measurement process performed by a transit-time ultrasonic anemometer is applied to a fluid flowing through a circular section pipe. This model considers the influence of the shift of the acoustic pulse trajectory from straight propagation due to the flow on the measured speed. The aim of this work is to estimate the errors induced in the measured velocity by the shift of the acoustic pulse trajectory. Using different duct's flow models, laminar and turbulent regimes have been analyzed. The results show that neglecting the effect of shift of the acoustic pulse trajectory leads to flow rate measurement underestimation.

List of symbols

A	cross-sectional area of the pipe
c	sound speed
$\csc(\phi)$	cosecant of ϕ angle
$\mathbf{C} = \{\mathbf{O},\xi,\zeta\}$	pipe coordinate system.
$\mathbf{C}_{\mathbf{S}}^{\mathbf{C}}$, $\mathbf{C}_{\mathbf{C}}^{\mathbf{S}}$	transformation matrices between **C** and **S**
C_2	coefficient of the measured velocity correction term
C_{20}	part of C_2 due to asymptotic expansion
C_{2s}	part of C_2 due to taking into account the deviation of the ray path from a straight line
d_c	duct cross-section diameter
K_h	hydraulic correction factor
l	length of measurement path
M	Mach number
n	exponent of Nikuradse velocity profile model
$\bar{Q}$	mean volumetric flow rate
Re	Reynolds number
$\mathbf{S} = \{\mathbf{O},x,z\}$	acoustic path coordinate system
u, w	components of the velocity profile inside the pipe expressed in **S** coordinate system
U, W	dimensionless components of the velocity profile inside the pipe expressed in **S** coordinate system
u_M	measured velocity along the measurement path
U_M	dimensionless measured velocity along the measurement path
$\boldsymbol{u}_\xi$	component of the measured velocity along the ξ axis
V_R	reference velocity
X, Z	dimensionless coordinates
Z_+, Z_-	deviation of the ray path from a straight line in forward and backward directions
Z_1	coefficient of M order term in the expressions of Z_+, Z_-
Z_2	coefficient of M^2 order term in the expressions of Z_+, Z_-
ν	fluid's cinematic viscosity
ϕ	measurement path inclination angle
υ	velocity profile inside the pipe expressed in **C** coordinate system
$\bar{\upsilon}$	average velocity across the cross-sectional area of the pipe

1 Introduction

Since 1940's, fluid velocity measurement techniques based on ultrasound are applied in many areas of the industry and engineering, like wind energy, wind engineering and medicine. Although there are various types of ultrasonic speedometer the most widely used type is the dual sensor transit-time type (Vaterlaus et al. 1999; Lynnworth 1989). It is a technique that measures the flow speed based on the detection of the influence of the flow field on the transmission of ultrasonic signals between a transmitter and a receiver. A pair of facing transducers defines a measurement path. The method allows estimating the velocity vector component parallel to the measurement path (or sonic path).

One of the most frequently applications of the acoustic measurement path shown in Fig. 1 is the ultrasonic flowmeter (Vaterlaus et al. 1999; Carlander and Delsing 2000). These devices determine the mean volumetric flow rate $\bar{Q} = \bar{v}A$ by measuring the mean velocity, $\bar{v}$, averaged across the pipe cross-section area, A.

There are various uncertainty sources associated to this measurement technique like the sonic path length and alignment, pipe geometry (Moore et al. 2000), kinetic turbulence (Andreeva and Durgin 2003), thermal turbulence (Iooss et al. 2002), flow profile (Moore et al. 2000; Olsen 1991; Yeh and Espina 2001) or transit-time measurement (Vaterlaus et al. 1999). This paper analyzes other source of uncertainty: the shift of the trajectory of the ultrasonic pulse from the straight path caused by the velocity field. This phenomenon is a well-known source of error (Lynnworth 1989; Mylvaganam 1989), especially in measurements of gas flow at high speeds, such as those encountered in flare-gas flowmetering where the flow velocity may exceed 100 m/s. Flare systems can be found in offshore production platforms, refineries and chemical plants where, even though the flare happens during 5% of the production time, almost 90% of the gas is flared up in this conditions (Mylvaganam 1989). To compensate for the drift effect Mylvaganam (1989) proposes to change slightly windward the orientation of both transducers.

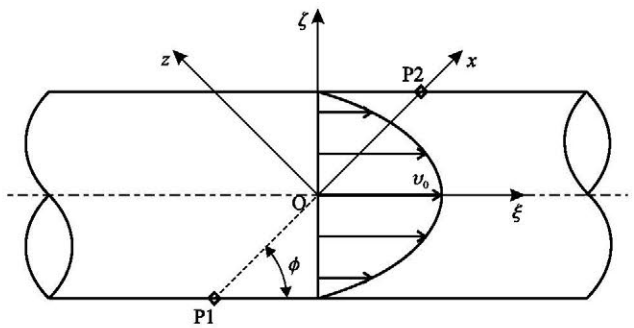

Fig. 1 Sketch of a flowmeter based on an ultrasonic measurement path. Duct reference frame (0,ζ,ξ). Measurement path reference frame (0,*x*,*z*). *P1, P2* ultrasonic transducers, ϕ path orientation angle

Later, this problem has been studied in several works where the equations of the geometrical acoustics are numerically solved for the propagation of the sound in a moving medium assuming different velocity profiles in the pipe. All of them used some iterative method to find out which ray ''hit'' on the receiver.

Yeh and Mattingly (1997) solved the equations for 11 analytical velocity profiles, and a velocity profile obtained with a CFD model. They found out that the deviation of the trajectory in both senses for non-uniform flows has S shape and its maximum deviation is in the order of the Mach number considered. In addition to this, they found that the error in the velocity measurement throughout the sonic path varies between 0 and –2%, depending on the velocity profile, the Reynolds and the Mach numbers considered.

Koechner and Melling (2000) used the statistical method of Monte Carlo to reduce the computer time requested to find the ray that reaches the receiver. Besides, they provided the intensity of the signal received, very useful information for the design of these devices.

More recently, Moore et al. (2002) numerically solved the equations of the geometrical acoustics using a 3°-order Runge-Kutta method combined with a bisection method to find the ray that gets to the receiver. They use a time-average turbulent velocity profile and then modulate on it random fluctuations of the speed whose root mean square distribution agree with values obtained in literature. Like Yeh and Mattingly (1997), Moore et al. (2002) presented trajectories with S shape between the transducers which maximum deviation was in the order of the Mach number considered and they found that the error in the speed measured depends on the Reynolds and the Mach numbers considered, obtaining a maximum error of 0.12% for Re = 22,494 and M = 0.1 in the case of time-averaged profile.

Likewise, Iooss et al. (2002) used a second-order Runge Kutta method to solve the geometrical acoustics equations and found out the ray that gets to the receiver by changing the output angle of the ray that leaves from the transmitter. They used the well-known model of Nikuradse as velocity profile. Applying the proposed method they calculated the error in the flow measurement for Re between 2.5×10^4 and 7.5×10^7, finding that it changes very little in the range of 0.3 and 0.4%. They also analyzed the effects of a temperature gradient, thermal turbulence and kinematic turbulence fields, finding errors in the flow measurement of approximately 1%.

Franchini et al. (2006), henceforth FSC, analyzed the wind speed measured using a dual sensor transit-time

ultrasonic anemometers considering the effect of the shift of the trajectory of the ultrasonic pulse from the straight line caused by the velocity field. The method was based on a mathematical model of the physical process of the ultrasound signal propagation between the transmitter and the receiver of the measurement path more advanced than the state-of-the-art models that consider just the straight path propagation (Kaimal et al. 1968; Silverman 1968; Kristensen and Fitzjarrald 1984; Cuerva et al. 2003). The mathematical model allows them to obtain the expressions of the transit-time of the ultrasound signal from the transmitter to the receiver, in both directions as a function of the velocity field and its derivatives. As it is well known the transit-time measurement starts when the acoustic signal is emitted by one transducer and it is finished when the opposite transducer detects the first arriving wave. Therefore, the problem consists in the determination of the minimum transit-time trajectory between the transducers. Thus, based on the geometrical acoustic and variational methods, forward and backward trajectories are determined and used for calculating the transit times in both directions. The expressions obtained help to determine the flow speed ''as given by the anemometer'', by applying the time inverse difference algorithm. One of the main conclusions of FSC's paper was that significative corrections of the measured speed may be needed in the case of rotational flows, where trajectory shifts are of the order of the flow Mach number.

As an application of the results obtained in the FSC paper, in this work the flow rate measurement inside a pipe is considered. This case has been selected because of both its scientific interest and its industrial applications, while it is also an example of rotational flow. The idea is to estimate the errors in the measurement of the mean velocity measured by an acoustic path due to the velocity profile in a configuration as shown in Fig. 1.

2 Flow in a circular cross-section duct

As the flow measurement is based on the velocity field along the measurement path between the ultrasonic transducers, a relation between the measured velocity along the measurement path, u_M, and the average speed, $\bar{v}$, has to be found. In the literature this relation is called ''hydraulic correction factor'' (Lynnworth 1989), defined as

$$K_h = \frac{\bar{v}}{u_\xi} = \frac{\bar{v}\cos\phi}{u_M}, \tag{1}$$

where u_ξ is the component of the measured velocity along the ξ axis (see Fig. 1). Some authors (like Iooss et al. 2002) prefer to use its inverse. Under the appropriate assumptions, which will be stated below, the estimation of K_h involves the evaluation of the modification of the measurement due to the shift of the acoustic pulse trajectory produced by the velocity field. It can be observed that the average velocity along the cross-section, $\bar{v}$, depends on the velocity profile, and therefore on the Reynolds number, $Re = \bar{v}d_c/\nu$, where d_c is the duct cross-section diameter and ν is the fluid's cinematic viscosity. Therefore, K_h is also a function of Re. Vaterlaus et al. (1999) studied this issue and gave two expressions for K_h, one valid for laminar regime ($Re < 2.600$) and the other one for turbulent flow ($Re > 4.000$). In these expressions the velocity measured by the anemometer u_M is considered to be the average of the path-wise speed component. The average speed over the cross-section, $\bar{v}$, is obtained from the integration of the velocity profile. For the laminar flow profile the authors use the Hagen–Poiseuille model to obtain the hydraulic correction factor

$$K_{hLR} = \frac{3}{4}, \tag{2}$$

where subscript L denotes ''laminar flow'' and subscript R the value to be used as reference for comparison with the results obtained with the models presented here. For turbulent flow these authors adopt the Nikuradse velocity profile model and obtain

$$K_{hTR} = (1.125 - 0.011\log Re)^{-1}, \tag{3}$$

where the subscript T means ''turbulent flow''.

To apply the hydraulic correction factor, the flow should be a completely developed one, that is, the measuring section should be placed far away from any perturbation such as valves, bents or section changes (Vaterlaus et al. 1999; Sanderson and Yeung 2002).

By using as reference speed $v_R = \bar{v}$ and Eq. 1 the hydraulic correction factor becomes

$$K_h = \cos\phi(U_M)^{-1}, \tag{4}$$

where U_M is the dimensionless measured velocity.

The theoretical model developed in the FSC's paper has been applied to determine the velocity which would be measured by an acoustic path, u_M, placed on a circular duct, both for laminar and turbulent flow conditions. Then, from the measured velocity, u_M, the enhanced hydraulic correction factors K_{hL} and K_{hT} are obtained, which takes into account the trajectory shift.

Analyzing the configuration shown in Fig. 1 where the acoustic measurement path is placed at an angle ϕ with regard to the duct axis, inside a meridian plane, it is

assumed that the measurement path is placed in a region of the duct where the flow is considered to be fully developed and steady (in the case of turbulent flow, the average velocity values are used). The mean flow is symmetric around the duct axis and therefore the azimuthal component is zero. The radial velocity component is neglected. The axial velocity component depends only on the radial coordinate, and its variation depends only on the flow regime (either laminar or turbulent).

The reference frames used are shown in Fig. 1: (1) the duct reference frame $\mathbf{C} = \{O,\xi,\zeta\}$ is fixed to the duct, ξ axis along the duct and ζ axis in the radial direction, with the origin at the center of the tube, and (2) the acoustic path reference frame, $\mathbf{S} = \{O,x,z\}$, x axis along the path and z axis perpendicular to x axis and inside the meridian plane. The origin is placed at the middle of the measurement path. The coordinates in both reference frames are related by the transformation matrices $\mathbf{C}_\mathbf{S}^\mathbf{C}$ and $\mathbf{C}_\mathbf{C}^\mathbf{S}$ as follows:

$$\begin{Bmatrix} x \\ z \end{Bmatrix} = \mathbf{C}_\mathbf{C}^\mathbf{S} \begin{Bmatrix} \xi \\ \zeta \end{Bmatrix}, \quad \begin{Bmatrix} \xi \\ \zeta \end{Bmatrix} = \mathbf{C}_\mathbf{S}^\mathbf{C} \begin{Bmatrix} x \\ z \end{Bmatrix}, \tag{5}$$

where

$$\mathbf{C}_\mathbf{S}^\mathbf{C} = \begin{bmatrix} \cos\phi & -\sin\phi \\ \sin\phi & \cos\phi \end{bmatrix}, \quad \mathbf{C}_\mathbf{C}^\mathbf{S} = \begin{bmatrix} \cos\phi & \sin\phi \\ -\sin\phi & \cos\phi \end{bmatrix}. \tag{6}$$

Following a description of the velocity profiles considered is presented, the applications to laminar and turbulent flow regimes are described, the results are shown, and finally conclusions are drawn.

3 Measurement in laminar flow regime (Hagen–Poiseuille flow)

In this section the case of the laminar flow in pipes is analyzed. We look for an expression of ''hydraulic correction factor'' based on the theoretical model developed in FSC's paper. The aim is to compare the data collected with this model, that considers the deviation of the trajectory of the ultrasound pulse, with the results found in literature, like the presented in the Eq. 2 (Vaterlaus et al. 1999) that does not consider the deviation of the ultrasonic pulse.

For Reynolds numbers less than some critical value, Re_{CR}, the flow can be considered laminar. Reported values of Re_{CR} in ducts vary from 2,300 to 2,600 (Schlichting 1979; Vaterlaus et al. 1999). The Hagen–Poiseuille profile of radial variation of speed is given by

$$v(\zeta) = v_0 \left[1 - \left(\frac{\zeta}{r_c}\right)^2\right], \tag{7}$$

where r_c is the duct radius and v_0 is the maximum speed $v_0 = v(0)$. The average speed across the cross-section is

$$\overline{v} = \frac{2\pi}{A} \int_0^{r_c} v(\zeta)\, \zeta \mathrm{d}\zeta = \frac{v_0}{2}, \tag{8}$$

where A is the cross-sectional area of the duct.

The velocity field, given in the duct reference frame (v, 0) should be written in the path reference frame by using the coordinate transformation matrix $\mathbf{C}_\mathbf{C}^\mathbf{S}$

$$\begin{Bmatrix} u \\ w \end{Bmatrix} = \mathbf{C}_\mathbf{C}^\mathbf{S} \begin{Bmatrix} v \\ 0 \end{Bmatrix}, \tag{9}$$

so that

$$\begin{aligned} u &= v_0 \left[1 - \left(\frac{x\sin\phi + z\cos\phi}{r_c}\right)^2\right] \cos\phi, \\ w &= -v_0 \left[1 - \left(\frac{x\sin\phi + z\cos\phi}{r_c}\right)^2\right] \sin\phi. \end{aligned} \tag{10}$$

By using dimensionless variables, $X = x/l$, $Z = z/l$ and $l = 2r_c/\sin\phi$, the dimensionless flow field in the path reference frame is given by

$$U(X,Z) = \frac{u}{v_R} = 2\cos\phi \left[1 - 4(X + Z\cot\phi)^2\right], \tag{11}$$

$$W(X,Z) = \frac{w}{v_R} = -2\sin\phi \left[1 - 4(X + Z\cot\phi)^2\right]. \tag{12}$$

The dimensionless rotational of the velocity field along the measurement path is

$$\frac{\partial U}{\partial Z}(X,0) - \frac{\partial W}{\partial X}(X,0) = U_{Z_0} - W_{X_0} = -\frac{16}{\sin\phi} X. \tag{13}$$

From the results of the FSC's paper, the deviation of the ray path from a straight line in forward and backward directions are given by $Z_+ = MZ_1 + M^2Z_2$ and $Z_- = -MZ_1 + M^2Z_2$, respectively, where Z_1 and Z_2 are the results of the problems

$$\text{order } M^1 : Z_1'' + (U_{Z_0} - W_{X_0}) = 0, \tag{14}$$

$$\begin{aligned} \text{order } M^2 : {} & Z_2'' - 2(U_0 U_{Z_0} + W_0 W_{Z_0}) + U_0 W_{X_0} \\ & + Z_1(U_{ZZ_0} - W_{XZ_0}) = 0, \end{aligned} \tag{15}$$

where

$$U_0 = U(X,0), \quad U_{Z_0} = \frac{\partial U}{\partial Z}(X,0), \quad U_{ZZ_0} = \frac{\partial^2 U}{\partial Z^2}(X,0),$$
$$W_0 = W(X,0), \quad W_{X_0} = \frac{\partial W}{\partial X}(X,0), \quad W_{Z_0} = \frac{\partial W}{\partial Z}(X,0),$$
$$W_{XZ_0} = \frac{\partial^2 W}{\partial X \partial Z}(X,0). \tag{16}$$

The velocity field and its derivatives along the measurement path in Eqs. 14 and 15 are determined with the help of Eqs. 11 and 12. Substituting their values in Eqs. 14 and 15 the differential equations for Z_1 and Z_2 are obtained:

$$Z_1'' - \frac{16}{\sin\phi} X = 0, \tag{17}$$

$$Z_2'' + R\left(X - 4X^3\right) = 0, \tag{18}$$

where

$$R = \frac{32}{3}\cot\phi\left(6 + \csc^2\phi\right) + 16\sin 2\phi. \tag{19}$$

The solutions of Eqs. 17 and 18 with the boundary conditions $Z_1(\pm\ 1/2) = Z_2(\pm\ 1/2) = 0$ are, respectively,

$$Z_1 = -\frac{2}{3\sin\phi}\left(X - 4X^3\right), \tag{20}$$

$$Z_2 = \frac{\mathrm{R}}{240}\left(7X - 40X^3 + 48X^5\right). \tag{21}$$

A typical trajectory shift is shown in Fig. 2, with the contributions of M and M^2 terms outlined. According to the solution of the problem given in the FSC's paper the measured velocity is

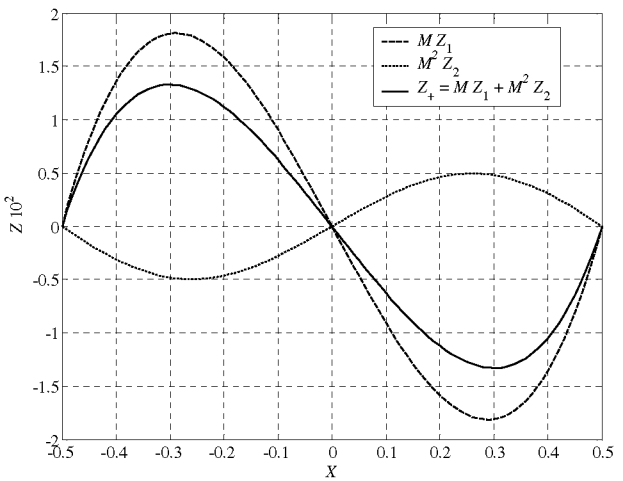

Fig. 2 Ultrasound pulse trajectory in the forward direction ($P1$ to $P2$) (*solid line*). $M = 0.1$, $\phi = 45°$. Contributions of the MZ_1 term (*dashed line*) and of the M^2Z_2 terms (*dotted line*). Laminar flow

$$U_{\mathrm{M}} = \overline{U_0}\left(1 + C_2 M^2\right), \quad C_2 = C_{20} + C_{2\mathrm{s}}, \tag{22}$$

where, with the help of the formulation summarized in the Appendix, the values of the parameters involved are determined as follows:

$$\overline{U_0} = \frac{4}{3}\cos\phi, \tag{23}$$

$$C_{20} = \overline{U_0}^2 - 2\overline{U_0^2} + \frac{\overline{U_0^3}}{\overline{U_0}} = \frac{16}{63}\cos^2\phi, \tag{24}$$

$$C_{2\mathrm{s}} = \frac{I_{G_3}}{\overline{U_0}} - 2I_{G_2} = -\frac{16}{105}\left(15 - 17\cos 2\phi + 4\cos 4\phi\right)\csc^2\phi. \tag{25}$$

Observe in Eq. 22 that the relative difference between the average of the path-wise velocity component $\overline{U_0}$ and the velocity measured by the anemometer, U_{M}, according to the model presented here, is C_2M^2. The order of magnitude of the correction can be of the square of the Mach number, M^2, so that, in the case of liquids, where $c \sim 10^3$ m s^{-1}, this correction might not be taken into account.

In order to evaluate its influence, the variation of the correction coefficients C_2, C_{20} and $C_{2\mathrm{s}}$ with the angle ϕ is shown in Fig. 3. The main contribution to C_2 comes from the term associated to the effect of the shift of the trajectory, $C_{2\mathrm{s}}$. The total correction C_2 is negative, so that the measured speed is smaller than the mean speed along the straight line. The minimum value of the correction is $C_2 = -2.5$ for a path orientation angle $\phi = 30°$.

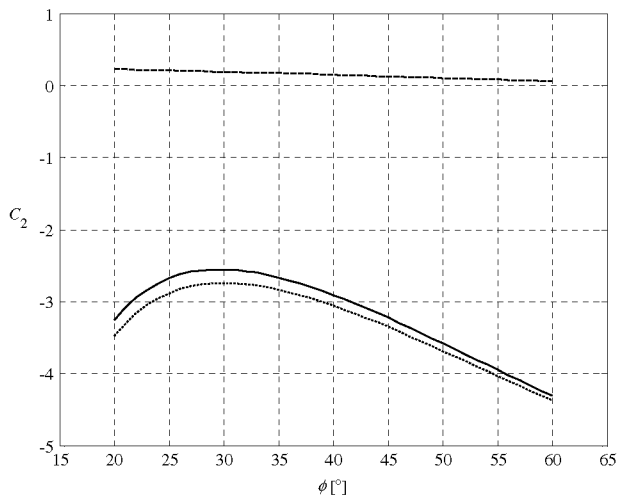

Fig. 3 Variation of the correction term, C_2, of the measured velocity with the path orientation angle ϕ (*solid line*). Contributions of the trajectory shift (*dotted line*) and speed non-uniformity (*dashed line*). Laminar flow

By using Eqs. 4 and 22, the enhanced laminar hydraulic correction factor is obtained:

$$K_{\mathrm{hL}} = \frac{3}{4}\left[1 - \frac{2\csc^2\phi}{315}(355 - 408\cos 2\phi + 101\cos 4\phi)M^2\right]^{-1}. \tag{26}$$

Observe the differences between this expression (which includes the effect of the trajectory shift) and the classical one, which only considers the average velocity along the straight line joining the transducers. The relative difference is defined as

$$\delta K_{\mathrm{hL}} = \frac{K_{\mathrm{hLR}} - K_{\mathrm{hL}}}{K_{\mathrm{hL}}} = C_2 M^2 = -\frac{2\csc^2\phi}{315}(355 - 408\cos 2\phi + 101\cos 4\phi)M^2. \tag{27}$$

The variation of δK_{hL} as a function of M is shown in Fig. 4, for several values of the path orientation angle ϕ. Observe that δK_{hL} is always negative. This implies that $K_{\mathrm{hL}} > K_{\mathrm{hLR}}$ and, therefore, when the flow rate (or $\bar{v}$) is determined by using Eq. 1, the value of $\bar{v}$ obtained with K_{hLR} is smaller than the ''correct'' value, the one obtained by using the enhanced value, K_{hL}. This effect increases when the Mach number M increases. The smallest correction appears when the orientation angle is $\phi \cong 30°$.

4 Measurement in turbulent flow regime

The velocity profile inside a circular cross-section duct is given by the Nikuradse model (Schlichting 1979; Vaterlaus et al. 1999) as

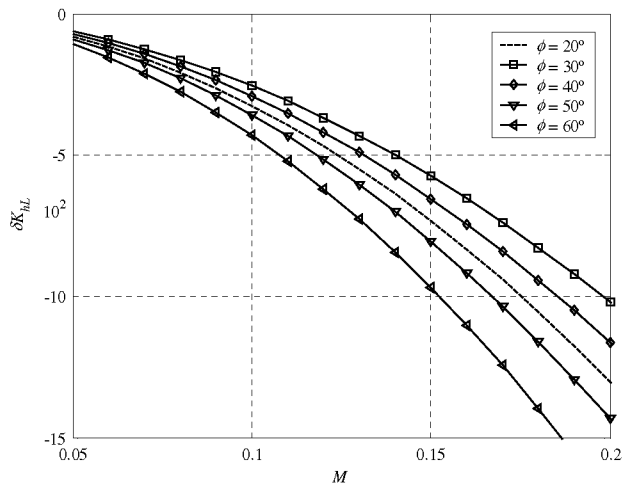

Fig. 4 Variation of the correction factor difference, δK_{hL}, with the Mach number, M. ϕ is the path orientation angle. Laminar flow

$$v(\zeta) = v_0\left(1 - \frac{|\zeta|}{r_c}\right)^{\frac{1}{n}}, \tag{28}$$

where r_c is the duct radius, and the exponent n is given by

$$\frac{1}{n} = 0.2525 - 0.0229\log Re, \quad 4 \times 10^3 < Re < 3.2 \times 10^6. \tag{29}$$

This model is widely employed in industrial applications. By using Eq. 28, the average velocity along a cross-section is

$$\bar{v} = \frac{2\pi}{A}\int_0^{r_c} v(\zeta)\,\zeta \mathrm{d}\zeta = v_0\frac{2n^2}{(n+1)(2n+1)}, \tag{30}$$

which is used as reference speed, v_{R}. Following a process like the one for the laminar flow, the dimensionless velocity field in the path reference system is

$$U = N_{\mathrm{R}}\cos\phi[1 - 2|X + Z\cot\phi|]^{\frac{1}{n}}, \tag{31}$$

$$W = -N_{\mathrm{R}}\sin\phi[1 - 2|X + Z\cot\phi|]^{\frac{1}{n}}, \tag{32}$$

where

$$N_{\mathrm{R}} = \frac{(n+1)(2n+1)}{2n^2}. \tag{33}$$

The azimuthal component of the rotational of the velocity field along the measurement path is

$$U_{Z_0} - W_{X_0} = -\mathrm{sgn}(X)\frac{2N_{\mathrm{R}}}{n\sin\phi}(1 - 2|X|)^{\frac{1-n}{n}}, \tag{34}$$

where sgn(X) denotes the sign of X.

The trajectory is obtained from Eqs. 14, 15, 31, 32 and 34. Calculations are more complex than in the case of laminar regime because of the modulus function in Eqs. 31 and 32. Details are not included here, but interested readers can ask for more detailed presentation of results and calculation to the authors.

Results concerning the drift of the trajectory are shown in Fig. 5. The contributions of order M and order M^2 terms are outlined, the most important being the contribution from order M term.

Following the procedure summarized in the Appendix, the measured speed can be written as

$$U_{\mathrm{M}} = \overline{U_0}(1 + C_2 M^2), \quad C_2 = C_{20} + C_{2s}, \tag{35}$$

where

$$\overline{U_0} = \left(1 + \frac{1}{2n}\right)\cos\phi, \tag{36}$$

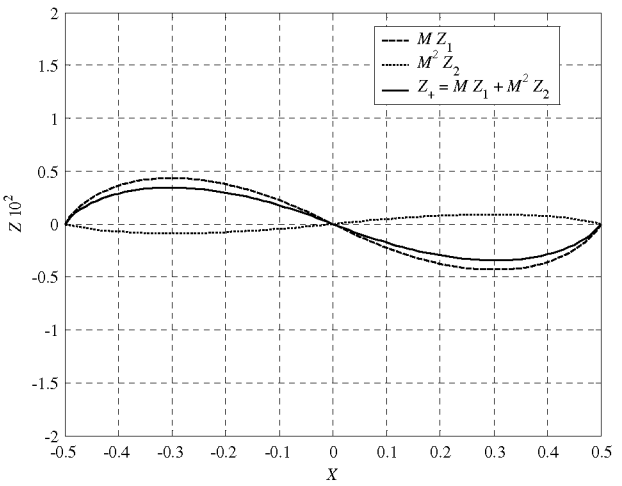

Fig. 5 Ultrasound pulse trajectory in the forward direction (*solid line*). $M = 0.1$, $\phi = 45°$, $n = 6$ ($Re = 5.6 \times 10^3$). Contributions of the MZ_1 term (*dashed-line*) and M^2Z_2 term (*dotted line*). Turbulent flow

and C_2 is obtained from Eqs. A2, A3 and A4, with

$$\overline{U_0^2} = \frac{nN_R^2 \cos^2\phi}{n+2}, \tag{37}$$

$$\overline{U_0^3} = \frac{nN_R^3 \cos^3\phi}{n+3}, \tag{38}$$

$$I_{G_2} = \frac{(2n+1)^2}{8n^3(n+2)}\left\{(n+1)^2\sin^2\phi + \frac{(n+2)}{\tan^2\phi} \times \left[F\left(1,-\frac{1}{n},2+\frac{1}{n},1\right)-1\right]-1\right\}, \tag{39}$$

$$I_{G_3} = \frac{(2n+1)^3}{32n^5(n+2)(n+3)}\left\{(n+2)(n+1)^3\cos 3\phi - (n+1)^2[n(n+3)+6]\cos\phi - \frac{4}{\tan\phi\sin\phi}[n(2n+5)+1]\right\}, \tag{40}$$

where F is the hipergeometric function.

The difference among the enhanced hydraulic correction factor K_{hT} and the reference factor K_{hTR} (considering the propagation along a straight line) is given by δK_{hT}

$$\delta K_{hT} = \frac{K_{hTR} - K_{hT}}{K_{hT}} = C_2 M^2. \tag{41}$$

The result is shown in Fig. 6. Observe that the correction is always negative, that is, the enhanced value is larger than the ''reference'' value. The use of the reference value instead of the enhanced value leads to underestimate the flow rate. According to Eq. 35 $C_2 = O(1)$ the correction of the velocity, U_M, is of order M^2. For a given orientation angle ϕ, the influence of the Reynolds number is not marginal, although the magnitude decreases as Re increases. In fact, the velocity profile becomes more uniform thus reducing the variance, and therefore decreasing the correction factor C_{20} (see Eq. A3 in Appendix).

In Fig. 7 the influence of the orientation angle ϕ in the correction factors C_{20} and C_{2s} is shown. Observe that the non-uniformity term C_{20} (which corresponds to the straight line trajectory) is almost constant and quite smaller than the effect produced by the shift of trajectory, C_{2s}.

In Fig. 8 the effect of Re on the difference of turbulent hydraulic correction factors δK_{hT} is shown, for several Mach numbers. The significant effect of the Mach number comes from the dependence of δK_{hT} on M, $\delta K_{hT} = C_2 M^2$, as explained before.

5 Conclusions

In this paper the FSC's model, devoted to the study of the effect of the shift of the pulse trajectory on the velocity measured by an ultrasonic measurement path, has been employed to determine the corrections to be taken into account in flowmeters based on ultrasonic measurement paths. In the published methods, the flow rate determination is based on the measurement of the average speed by an ultrasonic path, combined with a scaling factor so-called ''hydraulic correction factor'', for the laminar and turbulent regimes. These factors are based on assumptions concerning the radial variation of the axial velocity component across a section of the duct in each regime.

In this paper the difference between the velocity which would be measured by the anemometer considering the shift of the trajectory (with regard to the straight line) and

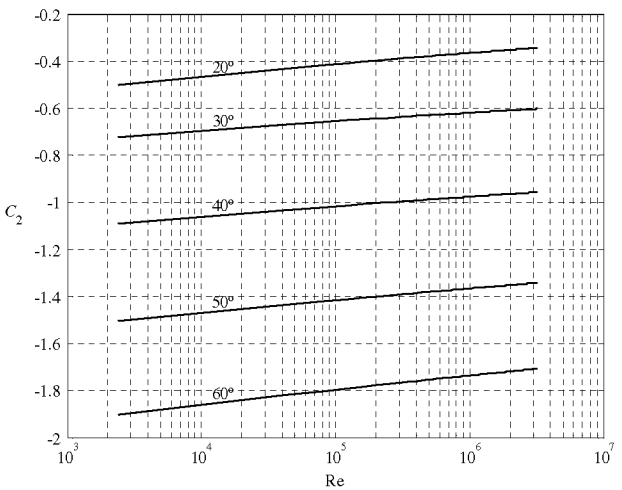

Fig. 6 Variation of the correction term C_2, with the Reynolds number, Re. Curves for five different path orientation angles, ϕ. Turbulent flow

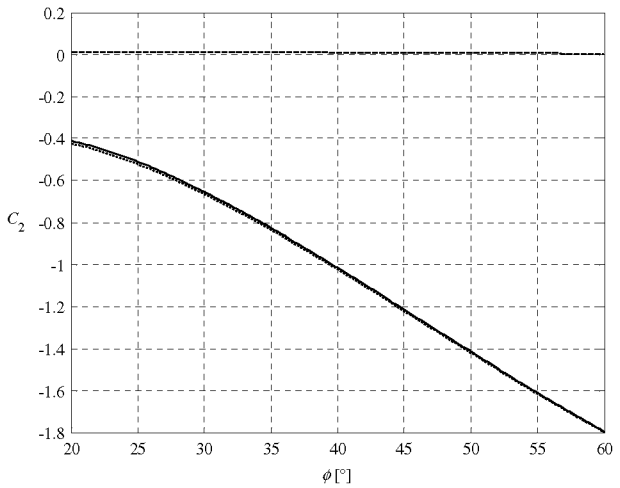

Fig. 7 Variation of the correction term, C_2, with the path orientation angle ϕ (*solid line*) for $Re = 1 \times 10^5$. Contributions of the trajectory shift (*dotted line*) and of the speed non-uniformity (*dashed line*). Turbulent flow

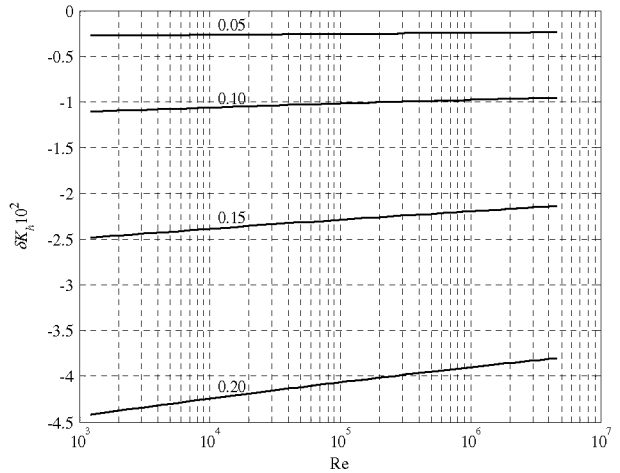

Fig. 8 Variation of the correction factor difference δK_{hT}, with the Reynolds number, *Re*. Legends indicate the value of the Mach number, *M*. The path orientation angle is $\phi = 40°$. Turbulent flow

the average velocity along the straight line trajectory has been determined for both laminar and turbulent radial profiles of the axial velocity component.

An analytical expression of the trajectories of the ultrasound signal has been found as much in laminar as in turbulent conditions. It is also shown that in both regimes the trajectories of the ultrasound signal have an S shape and the maximum shift is in the order of magnitude of Mach number. Similar results had been found by Yeh and Mattingly (1997) and Moore et al. (2002), although the velocity profiles considered by these authors are not as the ones considered in this paper.

In both regimes, it has been found that the measured speed (taking into account the trajectory shift) is larger than the one obtained by using the classical assumption (straight line trajectory). This implies that the use of hydraulic correction factor that can be found in the literature (Vaterlaus et al. 1999; Lynnworth 1989) underestimates the flow rate measurement.

The correction in the measured speed, M^2C_2, is mainly due to the trajectory shift, which therefore is dominant over the effect of the non-uniformity of velocity along the straight line trajectory. In the laminar case, the smallest correction appears when the path orientation angle is $\phi \cong 30°$.

In the turbulent regime, it has been found that the magnitude of the correction slowly increases with the Reynolds number, but the variation is faster with the orientation angle ϕ.

Appendix

According to Franchini et al. (2006), the measured speed is

$$U_M = \overline{U_0}\left(1 + C_2 M^2\right), \tag{A1}$$

where the correction term is given by

$$C_2 = C_{20} + C_{2s}, \tag{A2}$$

$$C_{20} = \overline{U_0}^2 - 2\overline{U_0^2} + \frac{\overline{U_0^3}}{\overline{U_0}}, \tag{A3}$$

$$C_{2s} = \frac{I_{G_3}}{\overline{U_0}} - 2I_{G_2}, \tag{A4}$$

by using

$$\overline{U_0} = \int_{-\frac{1}{2}}^{\frac{1}{2}} U_0 \mathrm{d}X, \quad \overline{U_0^2} = \int_{-\frac{1}{2}}^{\frac{1}{2}} U_0^2 \mathrm{d}X, \quad \overline{U_0^3} = \int_{-\frac{1}{2}}^{\frac{1}{2}} U_0^3 \mathrm{d}X,$$
$$I_{G_2} = \int_{-\frac{1}{2}}^{\frac{1}{2}} G_2 \mathrm{d}X, \quad I_{G_3} = \int_{-\frac{1}{2}}^{\frac{1}{2}} G_3 \mathrm{d}X, \tag{A5}$$

with the help of the auxiliary functions

$$G_2 = \frac{1}{2}\left(W_0 - Z_1'\right)^2 - Z_1 U_{Z_0}, \tag{A6}$$

$$G_3 = Z_1\left(2U_0 U_{Z_0} + W_0 W_{Z_0} - Z_1' W_{Z_0}\right) + Z_1'\left(Z_2' + U_0 W_0\right) - Z_2 U_{Z_0} - Z_2' W_0 - U_0 W_0^2. \tag{A7}$$

References

Andreeva TA, Durgin WW (2003) Ultrasonic thechnique for prediction of statistical characteristics of grid-generated turbulence. AIAA J 41(8):1438–1443

Carlander C, Delsing J (2000) Installation effects on an ultrasonic flow meter with implications for self diagnostics. Flow Meas Instrum 11:109–122

Cuerva A, Sanz-Andrés A, Navarro J (2003) On multiple-path sonic anemometer measurement theory. Exp Fluids 34:345–357

Franchini S, Sanz-Andrés A, Cuerva A (2006) Effect of the pulse trajectory on ultrasonic anemometer measurement. Exp Fluids (under review process)

Iooss B, Lhuillier C, Jeanneau H (2002) Numerical simulation of transit-time ultrasonic flowmeters: uncertainties due to flow profile and turbulence. Ultrasonics 40:1009–1015

Kaimal JC, Wyngaard J, Haugen D (1968) Deriving power spectra from a three-component sonic anemometer. J Appl Meteor 7:827–837

Koechner H, Melling A (2000) Numerical simulation of ultrasonic flowmeters. Acustica 86:39–48

Kristensen L, Fitzjarrald D (1984) The effect of line averaging on scalar flux measurements with a sonic anemometer near the surface. J Atmos Ocean Technol 1:138–146

Lynnworth LC (1989) Ultrasonic measurement for process control. Academic, London

Moore PI, Brown GJ, Stimpson BP (2000) Ultrasonic transit time flowmeters modeled with theoretical velocity profiles: methodology. Meas Sci Technol 11:1802–1811

Moore PI, Piomelli U, Johnson AN, Espina PI (2002) Simulations of ultrasonic transit-time in a fully developed turbulent flow meter using a Ray tracing method. In: North Sea flow measurement workshop, 22–25 October 2002

Mylvaganam K (1989) High-rangeability ultrasonic gas flowmeter for monitoring flare gas. IEEE Trans Ultrason Ferroelectr Freq Control 36(2):144–149

Olsen E (1991) An investigation of sonic and ultrasonic flowmeters with transducers in free stream. Flow Meas Instrum 2:185–187

Sanderson ML, Yeung H (2002) Guidelines for the use of ultrasonic non-invasive metering techniques. Flow Meas Instrum 13:125–142

Schlichting H (1979) Boundary-layer theory, 7th edn. McGraw-Hill, New York

Silverman B (1968) The effect of spatial averaging on spectrum estimation. J Appl Meteor 7:168–172

Vaterlaus HP, Hossle T, Giordano P, Bruttin C (1999) Ultrasonic flowmeters. In: Webster JG (ed) Measurement, instrumentation and sensors handbook. CRC, Boca Raton

Yeh TT, Espina PI (2001) Special ultrasonic flowmeter for in-situ diagnosis of swirl and cross flow. In: Proceedings of ASME FEDSM'01

Yeh TT, Mattingly (1997) Computer Simulation of Ultrasonic Flow meter performance in ideal an non-ideal pipeflows. In: Proceedings of ASME FEDSM'97